ACCSCIENCE PUBLISHING

Materials Science in Additive Manufacturing

ORIGINAL RESEARCH ARTICLE

Personalized antimicrobial and soundproof earplugs through embedded-suspension 3D printing of polydimethylsiloxane-Ag composites for the prevention of swimmers' otitis externa

Lili Qin[1*], Xinran Qian[1], Dengyun Xu[1], Jianming Yang[2], Junye Ren[1], Jialu Lu[2], Wenjia Zhang[1], Tianfeng Lu[1], Wenrui Wang[3*], and Ai Du[2*]

[1]Sports and Health Research Center, Department of Physical Education, Tongji University, Shanghai, China

[2]Shanghai Key Laboratory of Special Artificial Microstructure Materials and Technology, School of Physics Science and Engineering, Tongji University, Shanghai, China

[3]Anhui Provincial Key Laboratory of Tumor Evolution and Intelligent Diagnosis and Treatment, School of Life Sciences, Anhui Engineering Research Center for Neural Regeneration Technology and Medical New Materials, Bengbu Medical University, Bengbu, Anhui, China

***Corresponding authors:**
Ai Du
(duai@tongji.edu.cn)
Wenrui Wang
(2015003@bbmu.edu.cn)
Lili Qin
(qinlili@tongji.edu.cn)

Citation: Qin L, Qian X, Xu D, *et al*. Personalized antimicrobial and soundproof earplugs through embedded-suspension 3D printing of polydimethylsiloxane-Ag composites for the prevention of swimmers' otitis externa. *Mater Sci Add Manuf*. 2026;5(1):025260054. doi: 10.36922/MSAM025260054

Received: June 27, 2025

Revised: July 22, 2025

Accepted: July 25, 2025

Published online: October 6, 2025

Abstract

Aquatic activities, particularly swimming, have been demonstrated to enhance physical conditioning and psychological well-being. However, the risk of water-induced otitis externa—caused by microbial colonization in the external auditory canal—often deters sustained participation in aquatic sports. Traditional swimming earplugs are typically limited in terms of comfort, water resistance, and antimicrobial protection, which can lead to potential ear canal infections and reduced effectiveness in preventing water ingress. In this study, we proposed using 3D scanning and printing technology to produce personally customized swimming earplugs to address these challenges. Embedded-suspension 3D printing technology was applied to fabricate structures using non-self-supporting Polydimethylsiloxane (PDMS) ink, printing hydrophobic ink in a hydrophilic system. The 3D-printed PDMS/Ag-3% composites exhibited an excellent inhibition rate (99.89%), good sound insulation performance (>30 dB, 1000–6300 Hz, 8 mm thickness), elasticity (elongation at break of 62.93%), and low modulus (0.85 MPa). We then recruited 60 beginner swimmers for a wear trial to demonstrate the effectiveness of personalized earplugs in preventing otitis externa and reducing ear canal irritation. This approach not only highlights the potential of 3D printing technology in sports equipment but also offers new insights for developing customized wearables.

Keywords: 3D printing; Swimming earplugs; Swimmer's ear prevention; Sports equipment; Sports injury prevention

1. Introduction

Swimming and aquatic activities are integral to public health promotion, improving physical fitness, mental well-being, and social cohesion. However, swimming-induced ear pain has emerged as a significant health burden,[1,2] which may affect vulnerable populations and exacerbate health disparities.[3] When swimmers' ears are exposed to water, the moisture and water in the auditory canal can remove the protective lining and change the acidic environment of the ear canal to alkaline, thereby increasing susceptibility to infections.[4-9] Water safety is a critical public health priority. The Centers for Disease Control and Prevention highlights the importance of preventing swimming-related illnesses,[10] which not only compromise individual health but also impose substantial healthcare expenditure.[11,12] The economic burden extends beyond direct healthcare costs to include work and school absenteeism, as well as reduced participation in physical activities.[13,14] Therefore, it is vital to protect the health of swimmers when swimming in pools and public waters. Traditional swimming earplugs, typically made from silicone, wax, or foam, are designed for general use.[15] However, these earplugs often leave debris in the ear canal, increasing the risk of infection. In addition, traditional manufacturing processes restrict earplugs to standardized shapes, resulting in poor stability and limited antibacterial properties.[16]

In recent years, 3D printing technology has been increasingly applied in the modeling and preparation of new materials.[17] The flexibility of inks and materials, along with the ability to manipulate structures and functions, demonstrates great prospects across various fields.[18,19] Compared with traditional manufacturing processes, 3D printing technology demonstrates higher plasticity and flexibility, enabling the fabrication of complex structures.[20,21] Among the 3D printing techniques, embedded extrusion printing stands out as a promising method for fabricating complex 3D structures using low-modulus, low-viscosity, or slow-curing inks.[22-24] The suspension bath overcomes many limitations, including the dependence on support structures and nozzle clogging problems.[25-28] The application of 3D printing technology to fabricate swimming earplugs is not only cost-effective and easy to use but also allows for personalized designs tailored to the ear canal structures of swimmers and enthusiasts. Manufacturing earplugs that conform more closely to the auditory canal ensures enhanced stability and wearing comfort.

In terms of material selection, polydimethylsiloxane (PDMS) is a chemically stable, flexible, and biocompatible silicone macromolecular polymer material, which has a wide range of applications in flexible electronics,[29] medical devices,[30] and microfluidics.[31] Owing to the low elastic modulus of PDMS (≤1 MPa), it is often necessary to use support materials to maintain the stability of complex 3D structures.[32,33] Carbomer can be uniformly dispersed and stably suspended in liquid to form a high-viscosity gel,[34] which can provide a good supportive environment and ensure the uniform distribution of the printing material to enhance the printing accuracy and consistency. Concurrently, the gel strength and viscosity of carbomer can be precisely controlled by adjusting the concentration and pH to adapt to different printing requirements.[35] To further enhance the antimicrobial properties of the materials, silver (Ag), known for its antimicrobial effects, was incorporated to prepare novel PDMS-Ag composite inks. Ag is currently considered the most effective antibacterial metal. Silver ions (Ag^+) readily adsorb onto most bacterial biomolecules, disrupting their functions,[36] and this antimicrobial property is widely exploited in biomedicine, biomaterials, and medical implants.[37-39] The incorporation of Ag particles can significantly improve the mechanical properties of PDMS, complementing its inherent flexibility and elasticity. Slow sound propagation occurs in mixed structures, similar to aerogels.[40] High-density Ag particles combined with soft PDMS substrates may enhance the interaction between the material and sound waves, potentially improving sound insulation performance.[41]

In this study, we propose 3D-printed antimicrobial earplugs as both personal protective devices and scalable public health tools that provide an innovative solution to a common health issue faced by swimmers. The outer ear canal of each participant was modeled using an ear impression material and 3D scanning technology to create a personalized design. These custom swimming earplugs offer tailored protection during aquatic activities, reducing the risk of otitis externa. This aligns with the World Health Organization's (WHO) core principles of providing population-specific health solutions.[42] 3D-printed earplugs fabricated using suspension-embedded technology can be personalized and produced at a low cost, presenting an innovative solution aimed at preventing water-related ear infections and promoting safer aquatic activities. The key innovations in this study include (i) successful printing of hydrophobic PDMS ink within a hydrophilic support medium, enabling the creation of complex models without traditional molds and (ii) a dual-function design incorporating Ag, which imparts antibacterial properties to the composite material while enhancing its overall sound insulation performance.

2. Materials and methods

2.1. Materials

The PDMS material used was Sylgard 184 (Dow Corning), which was purchased from Merck Chemical Technology Co., Ltd. (China). Ag nanoparticles (200 nm), Carbomer 940, sodium hydroxide (NaOH), sodium chloride

(NaCl), and deionized water (DW) were purchased from Sinopharm Chemical Reagent Co., Ltd. (China); NaOH, NaCl, and DW were of analytical grade purity and used without further purification. LB broth and LB nutrient agar for biological experiments were purchased from Hope Biotechnology Co., Ltd. (China).

2.2. 3D printing of models

The earplug mold was first created using ear impression material, which was injected into the subject's external ear canal and quickly cured to obtain a personalized earplug size. This physical mold was then digitized using a 3D scanner, and the resulting model was optimized and styled using Rhino software (Figure 1). The 3D models, saved as Standard Triangle Language files, were converted to G-code and sliced into thick layers using Slic3r software integrated within the printing software (Cura Wiiboox). The resulting X3G file was then transferred to the 3D printer through an SD card.

2.3. Inks and support medium preparation

Pure PDMS ink is in a liquid state when extruded and requires prolonged curing at high temperatures (Figure 2A). Therefore, traditional direct-write 3D printing technology cannot produce complex structures using pure PDMS. The PDMS ink was prepared by mixing Sylgard 184 at a 10:1 base-to-curing-agent ratio. This mixture was stirred for 30 min using a mechanical mixer and then vacuum degassed for 20 min. The PDMS-Ag inks were prepared by mixing PDMS ink with Ag nanoparticles at different mass concentrations of 1%, 3%, 5%, and 10% relative to the total mass. Compared to pure PDMS ink, the PDMS-Ag ink requires ultrasonic dispersion for 30 min to evenly disperse the Ag nanoparticles before degassing. In preliminary experiments, we studied different carbomer formulations to optimize the NaOH concentration. Carbomer gels were prepared with 0, 0.40, and 0.60 g NaOH per 100 mL DW, while keeping Carbomer 940 fixed at 1.20 g. Pure carbomer has low yield stress and strong intermolecular forces, resulting in rheological properties unsuitable for printing. After adding NaOH, the carbomer molecular chains undergo stretching and crosslinking (Figure 2B), increasing the yield stress of the system to a suitable range for printing. The prepared mixture was then loaded into a sealed syringe for extrusion. The carbomer support bath was poured into a square container (side length = 4 cm) to hold the earplug construct during 3D printing and secured on the build platform.

2.4. Extrusion printing process

Figure 3A displays the 3D printing process for the personalized earplugs. A commercial fused deposition modeling 3D printer (One Mini, Wiiboox, China) was modified by incorporating an additional pressure-controlled regulator to precisely control the ink extrusion rate. Initially, when PDMS ink was injected into the pure

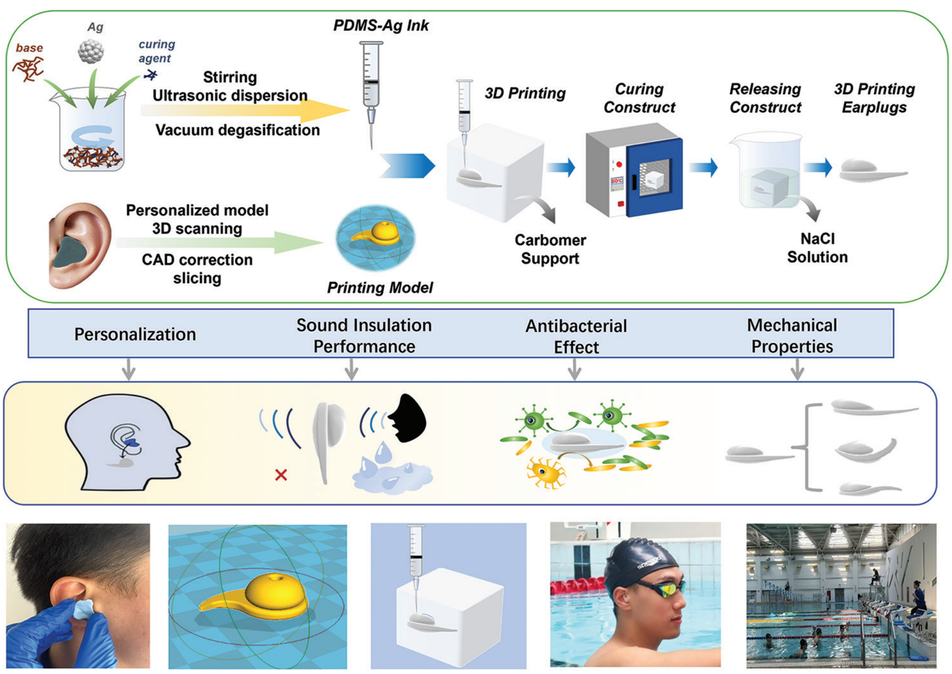

Figure 1. Synthesis and application of 3D-printed personalized earplugs
Abbreviations: CAD: Computer-aided design; PDMS: Polydimethylsiloxane

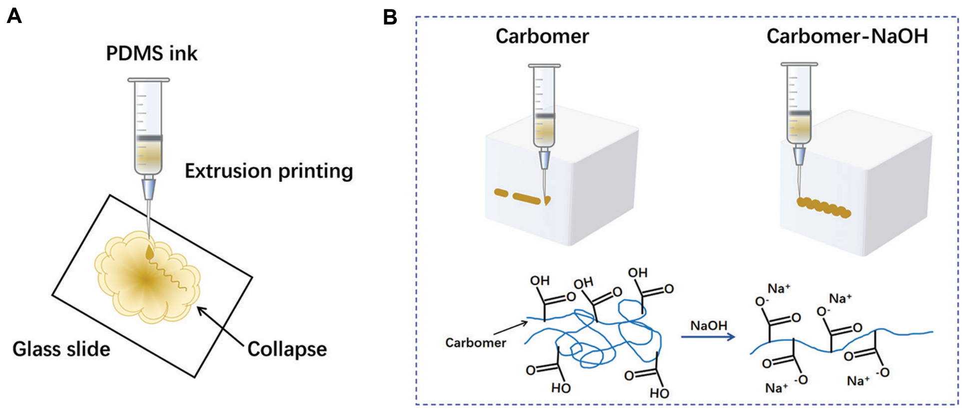

Figure 2. 3D printing with PDMS ink. (A) Polydimethylsiloxane (PDMS) ink in direct-write 3D printing. (B) PDMS ink in embedded-suspension 3D printing

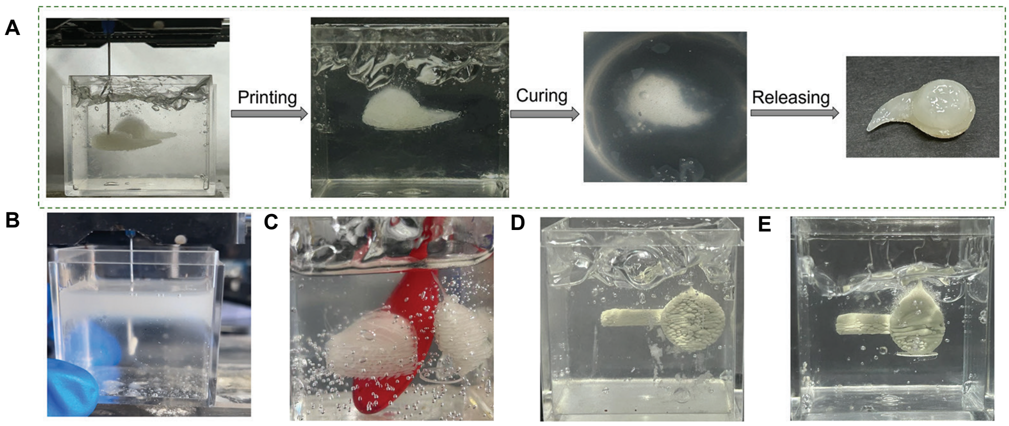

Figure 3. 3D printing process. (A) 3D-printed earplug process. (B) Extrusion in pure carbomer solution. (C) Curing of Polydimethylsiloxane (PDMS) in carbomer. (D and E) Print structure under different printing parameters: Printing with 80% fill density (D); and with other parameters unchanged, the upper layer: 0.15 mm layer height, and the lower layer: 0.20 mm layer height (E)

carbomer solution, it formed droplets near the needle tip and adhered to the needle surface (Figure 3B). After parameter adjustment, PDMS ink was successfully extruded as smooth, continuous, fine filaments within the carbomer matrix (Figure 3C), establishing the foundation for subsequent 3D structure printing. Figure 3D illustrates the outcome of suboptimal print parameters, specifically high layer height (>0.15 mm), low pressure (<40 psi), and low fill density (<80%), which lead to discontinuous ink deposition in the support structure. This results in an unstable printed form that fails to solidify properly and cannot be successfully removed. In contrast, the upper half of the features structure (Figure 3E) was printed with optimized parameters: layer height of 0.15 mm, 85% infill density, 25 mm/s print speed, and 50 psi extrusion pressure; these settings yielded dense, continuous filaments. However, when the layer height was reduced to 0.02 mm while keeping the other parameters constant, the resulting structure was sparse and poorly fused. These observations highlight how careful adjustment of printing parameters significantly enhances printing fidelity, improving both layer-to-layer bonding and structural integrity.

2.5. Curing and releasing the construct from the support medium

The construct, embedded within the carbomer support gel, was cured in a vacuum oven at 80°C for 24 h to ensure complete polymerization and formation of a stable elastomer. A flush solution was prepared by dissolving 2.338 g NaCl in 200 mL DW. After cooling, the construct was immersed in the flush solution for 20 min to remove the carbomer support. The remaining support material was easily removed through gentle rinsing, leaving behind the printed structure with high fidelity and minimal residual material.

2.6. Characterization

The rheological behaviors of the inks and the support medium were analyzed using a rotational rheometer

(HAAKE MARS 40, Thermo Scientific, Germany). Apparent viscosity was measured under shear rate sweep mode, with the shear rate increasing from 0.001 to 1000 s^{-1}. Stress sweep tests were performed at a constant frequency of 1 Hz to determine the storage modulus (G′) and loss modulus (G′′) as functions of shear stress from 1 to 1000 Pa. All experiments were conducted at 25°C, within the instrument's Peltier temperature control range of −40–200°C. Triplicate measurements were performed for each ink formulation, and the initial data points were discarded to eliminate artifacts due to sample loading. The microscopic morphology and elemental distribution of the printed constructs were analyzed using scanning electron microscopy (SEM) (Sigma 300, ZEISS, Germany). The crystal structure and phase composition were measured using X-ray diffraction (XRD) (Ultima IV, Rigaku, Japan). The mechanical properties of PDMS-Ag composites were assessed using a universal mechanical testing machine (5982, INSTRON, United States of America [USA]). The acoustic insulation properties of the 3D-printed materials were determined using an impedance tube (Type-4206, Brüel & Kjær, Denmark), covering a frequency range from 500 to 6300 Hz. The contact angle was measured by contact angle analysis (DSA25, KRUSS, Germany). The antimicrobial effects of the materials were tested using the spread plate method, with *Staphylococcus aureus* as the test organism, incubated in contact with the materials.

2.7. Applications of the 3D-printed earplugs in swimming

2.7.1. Participants and sampling

Participants in this study were recruited from a junior swimming class and a swimming club at Tongji University, China. Baseline data were collected from 60 participants, including height, weight, swimming level, swimming frequency, ear health status, and physical fitness. A total of 60 young adults (34 males and 26 females) aged 18–24 years participated in this study. The mean age of males was 20.15 ± 1.28 years, while that of the females was 20.12 ± 1.24 years. From this pool, 32 participants were selected for a 7-week experimental study based on the following criteria: no prior swimming experience, good physical health, and a normal body mass index. This subgroup included 16 males (age: 20.3 ± 1.40 years; height: 1.76 ± 0.43 m; mass: 65.6 ± 6.4 kg) and 16 females (age: 20.3 ± 1.4 years; height: 1.65 ± 0.38 m; mass: 53.5 ± 4.9 kg), with all values presented as mean ± standard deviation.

Ethical approval for this study was obtained from the Ethics Committee of Tongji University (approval number: tjdxsr2025061). All procedures were conducted in accordance with the Declaration of Helsinki and relevant institutional guidelines.

2.7.2. Personalized earplug wearing experiment

A total of 60 participants were selected for the earplugs-wearing experiment. Following ear impression molding, 3D scanning, and 3D printing, each participant received a custom-fitted pair of earplugs tailored to the unique shape of their ear canal (Figure S1). All participants were instructed to wear the earplugs during a 1-h swimming session. Afterward, user satisfaction was assessed using a structured questionnaire based on a Likert scale. The questionnaire consisted of 8 questions, each rated on a 5-point scale: strongly agree (5), agree (4), neither agree nor disagree (3), disagree (2), and strongly disagree (1).

2.7.3. Seven-week swimming exercise with earplugs

A total of 32 screened participants were randomly divided into two gender-balanced groups: an earplug-wearing group and a non-wearing control group. Both groups completed a 1-h swimming session once a week over 7 weeks. During this period, the Likert scale questionnaire was administered to both groups in weeks 1, 4, and 7. The questionnaire was designed to assess the participants' physical and psychological safety experience.

2.7.4. Statistical analysis

Data collected from the questionnaires were analyzed using the Statistical Package for Social Sciences® Version 29 (IBM Corp., USA). Continuous variables were reported as mean ± standard deviation or as median with interquartile range (IQR; 25^{th}–75^{th} percentiles), depending on data distribution. The Mann-Whitney U test was used to analyze the differences between groups for continuous variables. The Friedman test was used to analyze the data differences at different time points. A two-tailed $p<0.05$ was considered statistically significant.

3. Results

3.1. Ink matrix and carbomer formulation

Inks containing 1% and 3% Ag exhibited good fluidity and uniform Ag distribution. However, at concentrations of 5% and above, the inks experienced rapid nanoparticle agglomeration, leading to heterogeneous Ag distribution and compromised print fidelity. PDMS could not be extruded smoothly in the pure carbomer solution, and excessive NaOH addition reduced the transparency of the carbomer solution and introduced numerous bubbles. To address this, the NaOH concentration was fixed at 0.01 M to ensure adequate neutralization of the carbomer and sufficient yield stress, while preventing viscosity loss and bubble defects caused by excessive alkali. The viscous colloidal gel support medium was prepared by mixing 0.04 g NaOH and 1.2 g carbomer in 100 mL DW. The mixture was stirred for 2 h using a mechanical mixer and subsequently stored at 2°C for 48 h to reduce bubble formation. Through systematic optimization of the carbomer formulation, we mitigated critical challenges, including compromised interfacial adhesion and delamination propensity, arising from hydrophilic-hydrophobic repulsion between the ink matrix and the support structure.

3.2. Printing parameters

The printing parameters were carefully optimized to accommodate the specific requirements of the PDMS-Ag composite ink and the carbomer support gel system. Printing was conducted at a controlled temperature of 25°C. The syringe needles used had an inner diameter (d) and length (l) of 410 and 13 mm, respectively. The extrusion pressure was maintained within the range of 40–60 psi, and the print speed was set at 25 mm/s to ensure smooth and consistent ink flow without causing excessive shear stress on the ink. Based on preliminary experiments and ink rheological behavior, a layer height of 0.15 mm and an infill density of 85% were adopted to provide structural support while minimizing material usage and print time.

3.3. Rheological behavior

The viscosity of the PDMS ink displayed three distinct regimens across the shear rate range (Figure 4A): an initial shear-thickening region characterized by increasing viscosity with shear rate, followed by a Newtonian plateau where viscosity remained relatively constant, and a shear-thinning region in which viscosity decreased with increasing shear rate. In contrast, the PDMS-Ag inks exhibited shear-thinning properties at the initial stage, transitioning to Newtonian fluid and later displaying shear-thinning properties similar to the pure PDMS ink. Notably, all inks used in this study demonstrated low static viscosities (<60 Pa·s).

All inks exhibited a loss modulus (G′′) greater than the storage modulus (G′) (Figure 4B). Overall, the incorporation of Ag particles increased the viscosity of the system compared to pure PDMS inks. However, when the amount of Ag particles was low (*i.e.*, PDMS/Ag-1%), the interparticle interactions were weak, resulting in minimal reinforcement of the matrix. In addition, the incorporation

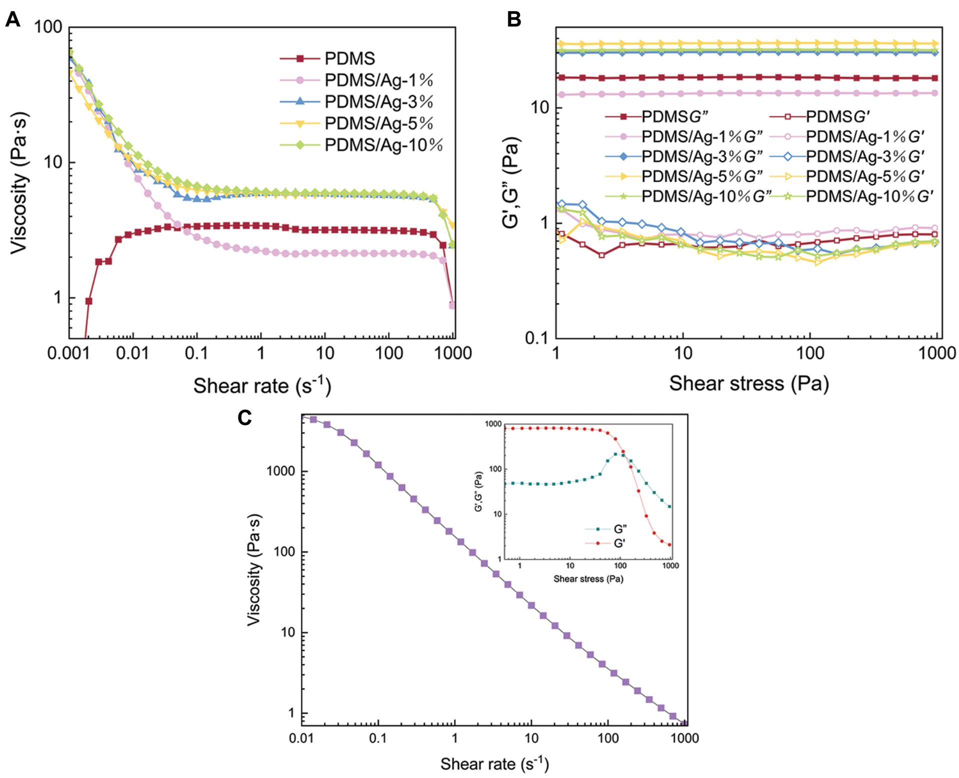

Figure 4. Rheological behaviors of the inks. (A) Apparent viscosity as a function of shear rate. (B) Storage (G′) and loss (G′′) moduli as a function of shear stress. (C) Rheological behavior of the carbomer solution
Abbreviation: PDMS: Polydimethylsiloxane

of Ag particles may have disrupted the original molecular chain mobility of the matrix, leading to a slight decrease in both modulus and viscosity. The differences in viscosity, G′, and G′′ of several other inks were relatively minor. Nevertheless, during the printing process, PDMS/Ag-5% and PDMS/Ag-10% exhibited poor stability due to the high concentration of Ag particles, which led to agglomeration, nozzle clogging, and the formation of intermittent filaments. Considering the overall rheological behavior and print performance, PDMS/Ag-3% was selected as the optimal ink formulation for 3D printing earplugs.

Carbomer solutions (Figure 4C) exhibited shear-thinning properties and rapid self-healing capabilities. Localized fluidization occurred when a needle applied stress while tracing across the supporting microgel, which rapidly returned to its original state when the needle was withdrawn. The viscosity of the carbomer support gel was modulated by adjusting its pH. We conducted several experiments to determine the optimal NaOH concentration, ensuring that the ink can spread effectively within the gel matrix for deposition, adhesion, and curing.

3.4. 3D-printed construct

3.4.1. Microstructural analysis

The SEM images of the samples (Figure 5A) indicated that the Ag nanoparticles have relatively smooth surfaces and are dispersed within the PDMS matrix as small-sized nanoparticles. The XRD spectra of Ag, PDMS-Ag, and PDMS are presented in Figure 5B. Ag exhibited characteristic diffraction peaks, suggesting that Ag has a face-centered cubic structure. Meanwhile, PDMS exhibited no distinct peaks, confirming it as a non-crystalline material.

3.4.2. Mechanical properties

Three independent samples ($n = 3$) were tested for tensile fracture and cyclic loading. To enhance clarity, representative curves from one sample are presented in Figure 6. The construct was stretched to fracture at a fixed rate of 10 mm/min, and the composites displayed approximately linear elastic behavior, with a maximum tensile strength of 0.52 ± 0.06 MPa and an elongation at break of 62.93 ± 3.8% (Figure 6A). The material exhibited good mechanical stability even after multiple stretch and compression cycles. The Mullins effect is most pronounced in the first loading cycle, with progressive stabilization after 3–5 cycles.[43] Accordingly, five consecutive loading-unloading cycles were applied to each PDMS-Ag sample to ensure that the material had reached a repeatable steady state. While the material exhibited plastic deformation in the first cycle, subsequent cycles demonstrated good elastic recovery (Figure 6B and C), indicating that the material possessed both elasticity and plasticity, enabling partial recovery of its original state, though some permanent deformation remains.

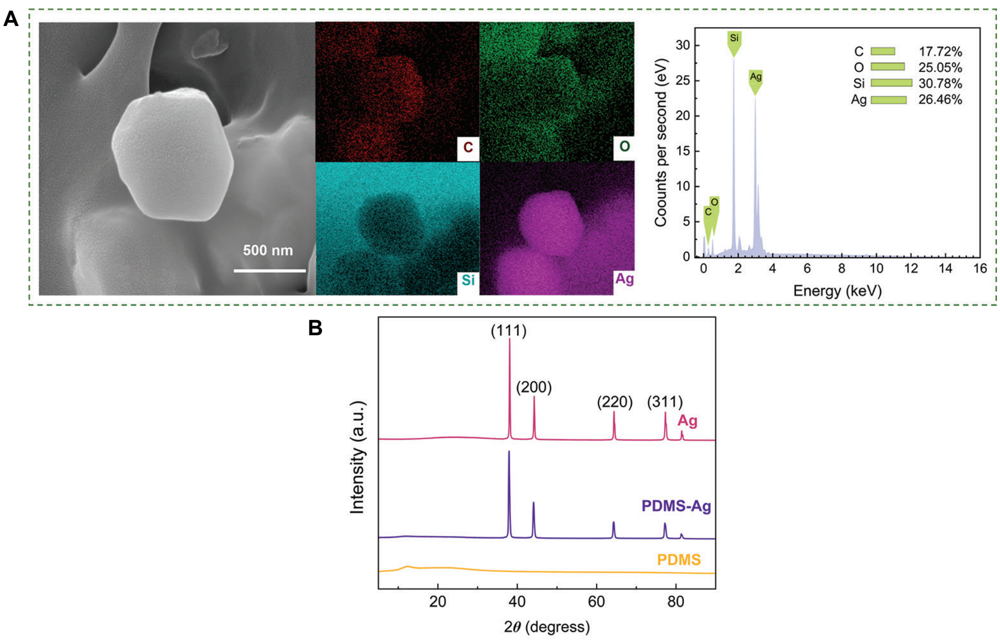

Figure 5. Microscopic morphology of the sample. (A) SEM images and EDS of the sample. (B) XRD patterns for Ag, PDMS-Ag, and PDMS. Scale bar: 500 nm (A)
Abbreviations: EDS: Energy dispersive spectroscopy; PDMS: Polydimethylsiloxane; SEM: Scanning electron microscope; XRD: X-ray diffraction

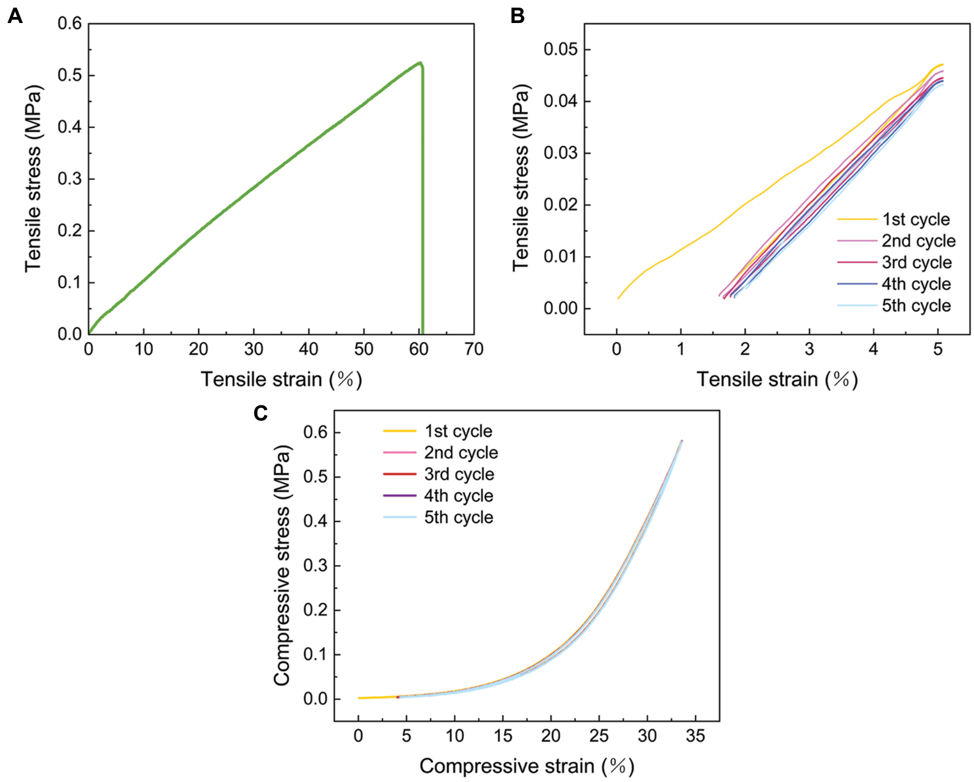

Figure 6. Mechanical properties of composites. (A) Tensile stress-strain of composites. (B) Tensile stress-strain curves of composites. (C) Compressive stress-strain curves of composites

3.4.3. Acoustic properties

Three independent PDMS-Ag earplugs were fabricated and tested. Figure 7 presents a representative sound insulation curve. The acoustic performance of PDMS-Ag composite samples (8 mm thickness; 29 mm diameter) was evaluated at a frequency range of 500–6300 Hz (Figure 7). The earplugs demonstrated excellent sound isolation at 1000–6300 Hz, achieving over 30 dB of sound insulation. Notably, at 4000 Hz, sound insulation ranged from 35.03 to 37.58 dB. Although the earplugs were less effective at blocking out low-frequency noises—such as human speech, which typically ranges from 85 and 255 Hz[44]—they outperformed most commercial swimming and sleeping earplugs. For comparison, typical silicone putty plugs offer ≈ 22 dB, wax plugs ≈ 25 dB, and polyurethane (PU)-foam plugs 29–32 dB. Compared to more airtight earplugs, the 3D-printed earplugs increase the swimmer's awareness of external warning sounds, further enhancing swimming safety.

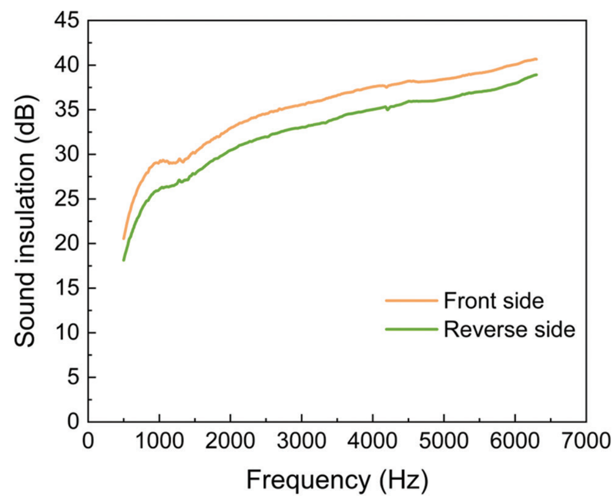

Figure 7. Sound insulation properties of polydimethylsiloxane-Ag composites. Front side refers to the upper surface; reverse side refers to the lower surface

The PDMS-Ag composite offers advantages in terms of mid- to high-frequency sound insulation and thickness efficiency, making it suitable for applications that require lightweight, flexible materials with wide-frequency noise reduction capabilities. These features may be attributed to the high impedance of Ag, which enhances interface reflection and inhibits sound wave transmission, thereby improving the sound insulation performance of PDMS-Ag composites. Table 1 presents the sound insulation values for various materials with different thicknesses reported in

Table 1. Sound insulation effects of different materials

Material	Sample thickness (mm)	Sound frequency (Hz)	Sound insulation capacity (dB)	References
PDMS-Ag	8	500–6300	−26−−38	This work
PDMS	5.08	1000	−29	45
PDMS-HGMs	5.08	1000	−26	45
Composite sound insulation structure	>50	1000	−35.1	46
Mineral wool panel	23	500–8000	−24−−30	47
Polyurethane foam panel	23	500–8000	−11−−30	47
	48	500–8000	−11−−32	48

Abbreviations: HGMs: Hollow glass microspheres; PDMS: Polydimethylsiloxane.

other studies. Although PDMS/HGM composite materials reduce thermal conductivity, they exhibit decreased sound insulation performance. In contrast, PU rubber focuses on low-frequency vibration reduction, while elastomer foam requires greater thickness to achieve broadband noise reduction.

3.4.4. Contact angle

The contact angle was measured at three distinct spots on a representative sample and averaged. As displayed in Figure 8, the droplet is fully absorbed by the material even after 100 s, and a higher receding contact angle of 95.64° was observed. In the context of swimming—where earplugs are used intermittently and are not exposed to water for prolonged periods—these properties indicate that the earplugs can maintain effective water resistance during typical swimming activities. In addition, the water droplets are less likely to stick to the surface, minimizing the scattering and absorption of sound waves, thereby allowing sound to be transmitted more clearly into the ear canal.

3.5. Antimicrobial performance of earplugs

The PDMS/Ag-1% formulation displayed no statistically significant antibacterial efficacy compared to the control group. In addition, further increasing the Ag content may increase material costs without significantly enhancing antibacterial efficacy. Therefore, the PDMS/Ag-3% formulation offered the best balance among antibacterial efficacy, printability, and cost effectiveness, and was selected as the representative composition. For each material type, three separate batches were produced, obtaining a total of nine samples. Each sample was co-cultured in LB broth, spread on three plates, and the average colony count was calculated (Figure 9A). Error bars in Figure 9B represent the standard deviation among the three averaged values per group. PDMS alone displayed no antibacterial activity and, in fact, slightly promoted bacterial growth compared to the LB blank control. Between pure PDMS and Ag, a highly significant difference was observed (***$p<0.001$), highlighting that pure Ag exhibits strong antibacterial effects. In repeated experiments, the colony-forming unit count for Ag was zero, with no significant variation across tests. However, the antibacterial effect of Ag was superior to that of PDMS-Ag, likely due to the encapsulation of Ag within PDMS reducing its antibacterial effect (Figure 9B). In summary, the PDMS/Ag-3% composite exhibited effective antimicrobial properties and meets the requirements for use in swimming earplugs.

3.6. User feedback on earplug wearability

Survey results (Figure 10) from 60 participants indicate that the 3D-printed swimming earplugs received high ratings across multiple dimensions, with average scores exceeding 4.0 for all questions. The mean score for satisfaction with appearance was 4.2, indicating that most respondents were satisfied with the earplugs' styling. High scores for non-allergic reaction (4.8) and comfort (4.1) emphasize the biocompatibility and safety of the material. Functional performance ratings focused on waterproofness (4.2) and acoustic isolation (4.0) further highlight the earplugs' effectiveness. The average score for no interference with swimming (4.0) and ear canal fit (4.1) highlights the benefits of personalized design. Notably, willingness to continue using the earplugs in the future scored 4.0, demonstrating a high level of user acceptance. Overall, these results validate that the 3D-printed swimming earplugs are a promising alternative to traditional earplugs, offering enhanced comfort and customization.

3.7. Effect of prolonged earplug use on swimmers over 7 weeks

The data analysis of 32 beginner swimmers (Table S1) revealed that the frequency of water entering the ear canal decreased in the group wearing earplugs compared to the non-wearing group starting from the 1st week. Significant differences were observed in weeks 4 and 7, indicating that the 3D-printed earplugs effectively reduce ear water ingress. In terms of underwater hearing, both groups had similar scores in recognizing external safety warning sounds, suggesting that the earplugs provide moderate isolation of the human voice and maintain good safety during swimming. In terms of concern about ear health, the wearing group exhibited a significant decrease after 7 weeks compared to the non-wearing group. In addition, the wearing group demonstrated better swimming

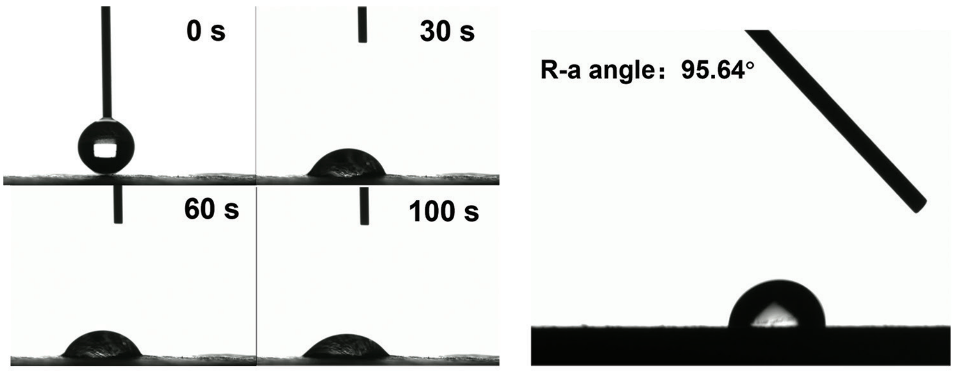

Figure 8. Water contact angle measurement of the construct
Abbreviation: R-a: Receding contact angle

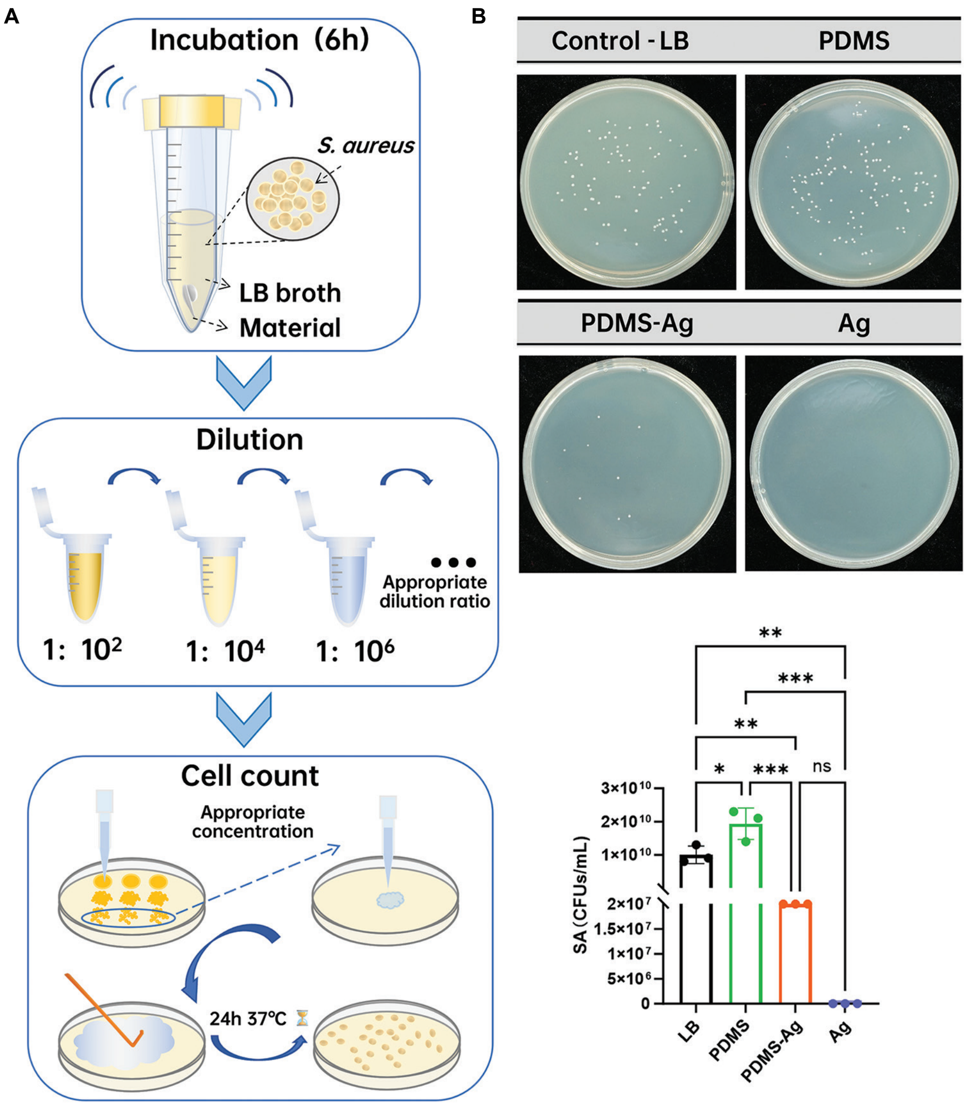

Figure 9. Antibacterial experiment on swimming earplugs. (A) Schematic workflow of the antibacterial activity test. (B) Antibacterial effects of different materials on *Staphylococcus aureus*; *p<0.05, **p<0.01, ***p<0.001, ns: p>0.05
Abbreviations: PDMS: Polydimethylsiloxane; SA: *Staphylococcus aureus*; CFU: Colony-forming Unit; LB: Luria-Bertani

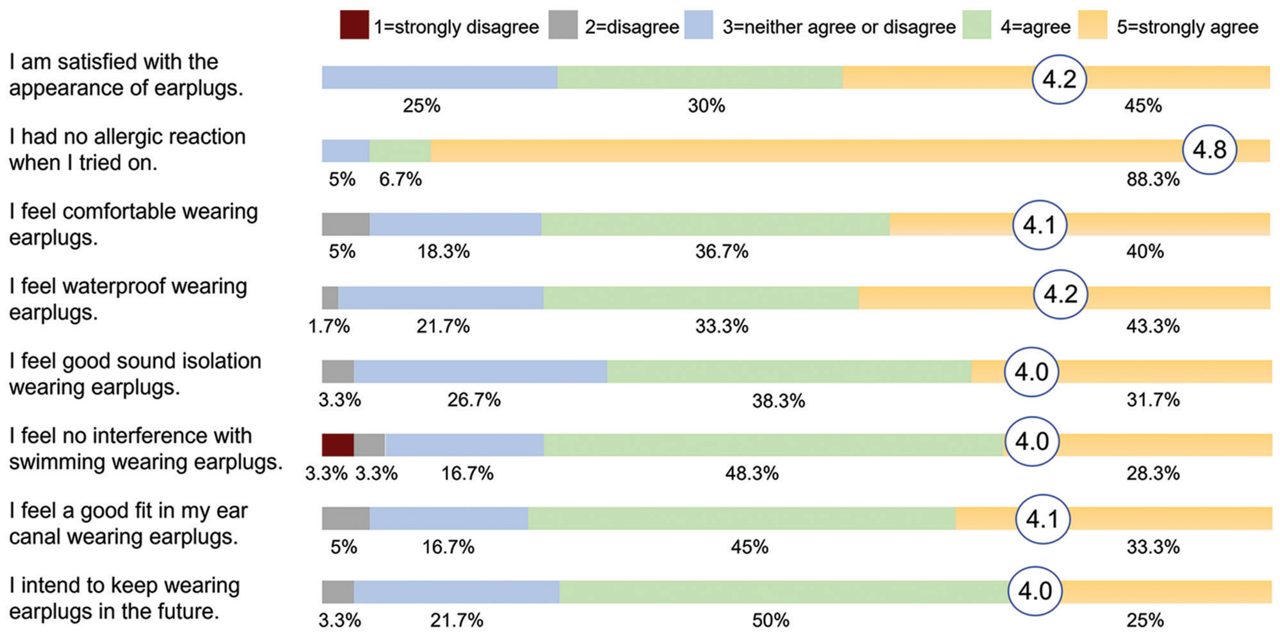

Figure 10. Likert scale for user feedback on earplug wearability (n = 60)

concentration than the non-wearing group during the 1st week of use.

4. Discussion

4.1. Superior performance of 3D-printed earplugs

The SEM, EDS, and XRD results collectively confirm that the PDMS-Ag composites were successfully fabricated, with Ag nanoparticles evenly distributed within the PDMS matrix. The overlapping curves (Figure 6B and C) after multiple cycles demonstrate good durability. For swimming earplugs, the resilience and durability of the material allow it to maintain a secure seal and comfort during repeated use while withstanding underwater pressure changes. Compared to soft silicone earplugs, these 3D-printed earplugs leave almost no debris in the ear canal after swimming. These earplugs performed well in insulating against medium- and high-frequency sounds but are less effective at blocking out low-frequency noises. In swimming environments, sounds such as splashing and underwater bubbles primarily occur above 1000 Hz, while human speech ranges between 85 and 255 Hz. These earplugs also effectively isolate underwater noise, providing swimmers with a comfortable swimming environment. Thus, the 3D-printed earplugs can increase the swimmer's awareness of external warning sounds, further enhancing swimming safety. In addition, the water droplets are less likely to stick to the surface of the earplugs, minimizing the scattering and absorption of sound waves to allow clearer sound transmission into the ear canal. Most literature addresses acoustic insulation and antimicrobial activity separately; however, our PDMS-Ag composite provides both effective sound insulation and broad-spectrum antibacterial effects, demonstrating a dual-function design ideal for swimming earplugs. Overall, users benefit from enhanced auditory clarity, which is especially important for underwater activities like swimming, where clear sound transmission is crucial for safety and communication.

4.2. Health promotion for swimmers wearing 3D-printed earplugs

The results for the non-wearing group revealed several improvements over the swimming period. Water comfort during swimming increased notably by weeks 4 and 7 compared to the initial week, indicating a growing adaptation to swimming activities. There was also a marked reduction in the incidence of water entering the ear canal by week 7, demonstrating an improvement in preventing water ingress over time. Underwater hearing, particularly in recognizing external safety warning sounds, significantly improved by week 7. Concerns regarding ear canal health decreased significantly at weeks 4 and 7, suggesting reduced anxiety about ear-related issues with continued swimming. This may be attributed to beginners' increasing adaptation to water exposure, leading to less frequent water ingress. Likewise, swimmers' anxiety levels decreased significantly by week 7, indicating greater overall comfort and confidence in the water. Furthermore, participants demonstrated improved concentration during swimming, with higher focus levels at weeks 4 and 7 compared to week 1, suggesting enhanced engagement and immersion as the swimming experience accumulated.

Over the 7-week experiment, the wearing group demonstrated significant improvements in water comfort and reduced ear canal water ingress (Table S2). Specifically, the frequency of water entering the ear canal decreased significantly during swimming. Concerns about ear canal health decreased significantly at weeks 4 and 7 compared to the initial week. Swimming anxiety also reduced over time, suggesting that wearing earplugs has a positive psychological impact on beginner swimmers. While overall swimming concentration remained relatively stable in the wearing group, participants wearing 3D-printed earplugs reported significantly higher concentration levels in the 1st week compared to the non-wearing group. These results highlight the positive impact of 3D-printed earplugs on swimmer comfort, ear protection, and psychological well-being over time.

4.3. Promotion of earplugs for swimming

Wearing personalized antibacterial earplugs can enhance public awareness of self-protection and increase enjoyment during aquatic activities. Through the 7-week experiment, participants in the wearing group demonstrated improved swimming safety awareness and developed long-term, effective health management habits. The promotion of swimming earplugs has significantly aided the public in learning the correct use of earplugs and other sports equipment. This has effectively prevented water ingress and ear infections, fostered awareness of safety and health, optimized swimming habits, and strengthened ear health protection. The promotion of earplugs also plays a valuable role in health monitoring and disease prevention. In future research, we envisage implanting smart sensors into 3D-printed structures to monitor vital signs, such as heart rate, ear health, and motion status.[48,49] By tracking physiological parameters, these devices can provide early warnings of potential health issues, such as infections and other illnesses, enabling timely medical intervention. Traditional silicone earplugs rely on injection molding,[16] which has limitations in terms of customizing the geometry of the individual ear canals. In contrast, we used embedded-suspension 3D printing technology to produce personalized earplugs that fit the user's ear canal without the need for molds. This innovation not only enhances personal health management but also contributes to safer and healthier swimming activities for the public in the future.

5. Conclusion

This study demonstrates the successful application of embedded 3D printing technology in developing personalized antimicrobial earplugs for swimming. The PDMS-Ag composite exhibited excellent rheological properties, inhibition rate (99.89%), and mechanical durability (elongation at break of 62.93%), enabling precise customization with high accuracy. The earplugs effectively block water ingress (water contact angle: 95.64°) while maintaining sound transmission in the 600–1000 Hz range, ensuring user safety and environmental awareness. Overall, this study highlights the feasibility and advantages of 3D printing technology for producing functional swimming accessories and offers innovative solutions for enhancing ear health protection in aquatic activities.

Acknowledgments

The authors would like to thank the Shanghai Key Laboratory of Special Artificial Microstructure Materials and Technology for providing the experimental conditions, as well as the students of the swimming class at Tongji University for their cooperation and support. The authors would like to acknowledge financial support from the Open Project of Anhui Engineering Research Center for Neural Regeneration Technology and Medical New Materials (AHNR2024Z002).

Funding

This work was supported in part by the Open Project of Anhui Engineering Research Center for Neural Regeneration Technology and Medical New Materials (AHNR2024Z002).

Conflict of interest

The authors declare that they have no competing interests.

Author contributions

Conceptualization: Lili Qin, Xinran Qian, Junye Ren
Data curation: Xinran Qian, Dengyun Xu, Junye Ren, Jianming Yang
Formal analysis: Xinran Qian, Jianming Yang, Junye Ren, Jialu Lu
Funding acquisition: Lili Qin
Investigation: Xinran Qian, Dengyun Xu, Jianming Yang, Junye Ren, Jialu Lu
Methodology: Wenrui Wang, Jianming Yang, Jialu Lu
Project administration: Wenjia Zhang, Tianfeng Lu
Supervision: Wenjia Zhang, Tianfeng Lu, Lili Qin
Writing–original draft: Lili Qin, Xinran Qian, Dengyun Xu
Writing–review & editing: Lili Qin, Ai Du, Wenrui Wang

Ethics approval and consent to participate

The study was conducted in accordance with the Declaration of Helsinki and approved by the Ethics Committee of

Tongji University (approval no. tjdxsr2025061; March 31, 2025).

Consent for publication

All participants agreed to participate in this study and provided verbal consent for the use of their data and images in publications.

Availability of data

All data generated or analyzed in this study are included in this article. Further inquiries can be directed to the corresponding authors.

References

1. DeFlorio-Barker S, Wing C, Jones RM, Dorevitch S. Estimate of incidence and cost of recreational waterborne illness on United States surface waters. *Environ Health*. 2018;17(1):3.

   doi: 10.1186/s12940-017-0347-9

2. Lipska J, Hamerska J, Hamerska L, *et al*. Swimmer's ear: Prevention, diagnosis, treatment, and management strategies for athletes. *Qual Sport*. 2024;18:53330.

   doi: 10.12775/QS.2024.18.53330

3. Perez-Stable EJ, Sayre MH. Reducing health disparities to promote health equity through policy research. *Ethn Dis*. 2019;29(S2):321-322.

   doi: 10.18865/ed.29.S2.321

4. Caramia G, Serafini V, Loggi A. The swimmer's otitis. An up to date and prevention options. *Pediatr Med Chir*. 2013;35(3):177-182.

   doi: 10.4081/pmc.2013.38

5. Strauss MB, Dierker RL. Otitis externa associated with aquatic activities (swimmer's ear). *Clin Dermatol*. 1987;5(3):103-111.

   doi: 10.1016/S0738-081X(87)80016-0

6. Beers SL, Abramo TJ. Otitis externa review. *Pediatr Emerg Care*. 2004;20(4):250-256.

   doi: 10.1097/01.pec.0000121246.99242.f5

7. Wang MC, Liu CY, Shiao AS, Wang T. Ear problems in swimmers. *J Chin Med Assoc*. 2005;68(7):347-352.

   doi: 10.1016/S1726-4901(09)70174-1

8. Kanagamuthu P, Dhanasekaran B, Karthika SR, Raghavan VK. To determine the pH of external auditory canal in otitis externa: A prospective observational study in a tertiary health care centre. *Indian J Otolaryngol Head Neck Surg*. 2023;75(1):502-506.

   doi: 10.1007/s12070-023-03591-x

9. Ellis J, De La Lis A, Rosen E, Simpson MTW, Beyea MM, Beyea JA. Approach to otitis externa. *Can Fam Physician*. 70(6):617-623.

   doi: 10.46747/cfp.7010617

10. World Health Organization. *Precision Public Health Strategy*. Brazzaville: WHO African Region; 2025. p. 2024-2030.

11. Wade TJ, Sams EA, Beach MJ, Collier SA, Dufour AP. The incidence and health burden of earaches attributable to recreational swimming in natural waters: A prospective cohort study. *Environ Health*. 2013;12(1):67.

    doi: 10.1186/1476-069X-12-67

12. Kumpel E, Delaire C, Peletz R, *et al*. Measuring the impacts of water safety plans in the Asia-Pacific region. *Int J Environ Res Public Health*. 2018,15(6):1223.

    doi: 10.3390/ijerph15061223

13. Bhatia R, Chauhan A, Rana M, Kaur K, Pradhan P, Singh M. Economic burden of otitis media globally and an overview of the current scenario to alleviate the disease burden: A systematic review. *Int Arch Otorhinolaryngol*. 2024;28(3):e552-e558.

    doi: 10.1055/s-0043-1767802

14. Graydon K, Waterworth C, Miller H, Gunasekera H. Global burden of hearing impairment and ear disease. *J Laryngol Otol*. 2019;133(1):18-25.

    doi: 10.1017/S0022215118001275

15. Mahboubi H, Lee A, Kiumehr S, Zardouz S, Shahriari S, Djalilian HR. Efficacy of commercial earplugs in preventing water intrusion during swimming. *Otolaryngol Head Neck Surg*. 2013;148(3):415-419.

    doi: 10.1177/0194599812471798

16. Chisholm EJ, Kuchai R, McPartlin D. An objective evaluation of the waterproofing qualities, ease of insertion and comfort of commonly available earplugs. *Clin Otolaryngol Allied Sci*. 2004;29(2):128-132.

    doi: 10.1111/j.1365-2273.2004.00795.x

17. Yang J, Lu J, Han D, Zhou B, Du A. Direct ink writing of aerogels: Fundamentals, strategies, applications, and perspectives. *Prog Mater Sci*. 2025;152:101462.

    doi: 10.1016/j.pmatsci.2025.101462

18. Yang J, Lu J, Xi S, *et al*. Direct 3D print polyimide aerogels for synergy management of thermal insulation, gas permeability and light absorption. *J Mater Chem A Mater Energy Sustain*. 2023;11(39):13.

    doi: 10.1039/D3TA02928J

19. Han D, Yang J, Wang H, *et al*. 3D-printed hybrid zirconia hydrogels for ultrahigh-efficiency phosphate adsorption. *Adv Compos Hybrid Mater*. 2024;7(4):1-14.

    doi: 10.1007/s42114-024-00941-3

20. Saadi M, Maguire A, Pottackal NT, *et al*. Direct ink writing: A 3D printing technology for diverse materials. *Adv Mater*.

2022;34(3):e2108855.

doi: 10.1002/adma.202108855

21. Walker DA, Hedrick JL, Mirkin CA. Rapid, large-volume, thermally controlled 3D printing using a mobile liquid interface. *Science.* 2019;366(6463):360-364.

doi: 10.1126/science.aax1562

22. Wu Q, Song K, Zhang D, *et al*. Embedded extrusion printing in yield-stress-fluid baths. *Matter.* 2022;5(11):3775-3806.

doi: 10.1016/j.matt.2022.09.003

23. Yang J, Qian X, Yang J, *et al*. Additive-free aerogel 3D printing using ultra-low storage modulus inks. *Adv Funct Mater.* 2024:2423739.

doi: 10.1002/adfm.202423739

24. McCormack A, Highley CB, Leslie NR, Melchels FPW. 3D printing in suspension baths: Keeping the promises of bioprinting afloat. *Trends Biotechnol.* 2020;38(6):584-593.

doi: 10.1016/j.tibtech.2019.12.020

25. Lee A, Hudson AR, Shiwarski DJ, *et al*. 3D bioprinting of collagen to rebuild components of the human heart. *Science.* 2019;365(6452):482-487.

doi: 10.1126/science.aav9051

26. Croom BP, Abbott A, Kemp JW, *et al*. Mechanics of nozzle clogging during direct ink writing of fiber-reinforced composites. *Addit Manuf.* 2021;37:101701.

doi: 10.1016/j.addma.2020.101701

27. Altıparmak SC, Yardley VA, Shi Z, Lin J. Extrusion-based additive manufacturing technologies: State of the art and future perspectives. *J Manuf Process.* 2022;83:607-636.

doi: 10.1016/j.jmapro.2022.09.032

28. Billiet T, Gevaert E, De Schryver T, Cornelissen M, Dubruel P. The 3D printing of gelatin methacrylamide cell-laden tissue-engineered constructs with high cell viability. *Biomaterials.* 2014;35(1):49-62.

doi: 10.1016/j.biomaterials.2013.09.078

29. Nathan A, Ahnood A, Cole M, *et al*. Flexible electronics: The next ubiquitous platform. *Proc IEEE.* 2012;100(SI):1486-1517.

doi: 10.1109/JPROC.2012.2190168

30. Gondil VS, Ashcraft M, Ghalei S, *et al*. Anti-infective bacteriophage immobilized nitric oxide-releasing surface for prevention of thrombosis and device-associated infections. *ACS Appl Bio Mater.* 2025;8(3):1362-1376.

doi: 10.1021/acsabm.4c01638

31. Wolf MP, Salieb-Beugelaar GB, Hunziker P. PDMS with designer functionalities-properties, modifications strategies, and applications. *Prog Polym Sci.* 2018;83:97-134.

doi: 10.1016/j.progpolymsci.2018.06.001

32. Duraivel S, Laurent D, Rajon DA, *et al*. A silicone-based support material eliminates interfacial instabilities in 3D silicone printing. *Science.* 2023;379(6638):1248-1252.

doi: 10.1126/science.ade4441

33. O'Bryan CS, Bhattacharjee T, Hart S, *et al*. Self-assembled micro-organogels for 3D printing silicone structures. *Sci Adv.* 2017;3(5):e1602800.

doi: 10.1126/sciadv.1602800

34. Hinton TJ, Hudson A, Pusch K, Lee A, Feinberg AW. 3D printing PDMS elastomer in a hydrophilic support bath via freeform reversible embedding. *ACS Biomater Sci Eng.* 2016;2(10):1781-1786.

doi: 10.1021/acsbiomaterials.6b00170

35. Fenny Indah S, Desy N, Dina F. Overview: Application of Carbopol 940 in Gel. In: *Proceedings of the International Conference on Health and Medical Sciences (AHMS 2020)*. Netherlands: Atlantis Press; 2021. p. 80-4.

36. Prasad SR, Teli SB, Ghosh J, *et al*. A review on bio-inspired synthesis of silver nanoparticles: Their antimicrobial efficacy and toxicity. *Eng Sci*. 2021;16:90-128.

doi: 10.30919/es8d479

37. Bhattacharjee T, Zehnder SM, Rowe KG, *et al*. Writing in the granular gel medium. *Sci Adv.* 2015;1(8):e1500655.

doi: 10.1126/sciadv.1500655

38. Mo F, Zhou Q, He Y. Nano-Ag: Environmental applications and perspectives. *Sci Total Environ.* 2022;829:154644.

doi: 10.1016/j.scitotenv.2022.154644

39. Yin IX, Zhang J, Zhao IS, Mei ML, Li Q, Chu CH. The antibacterial mechanism of silver nanoparticles and its application in dentistry. *Int J Nanomedicine.* 2020;15:2555-2562.

doi: 10.2147/IJN.S246764

40. Xie Y, Zhou B, Du A. Slow-sound propagation in aerogel-inspired hybrid structure with backbone and dangling branch. *Adv Compos Hybrid Mater*. 2021;4(8):248-256.

doi: 10.1007/s42114-021-00234-z

41. Borah B, Dash RK. Improved dielectric properties of rGO/PDMS composites by incorporation of Ag nanoparticles. *J Mater Sci Mater Electron*. 2022;33(15):12334-12350.

doi: 10.1007/s10854-022-08191-z

42. Centers for Disease Control and Prevention. *Preventing Swimming-Related Illnesses*; 2025. Available from: https://www.cdc.gov/healthy-swimming/prevention/index.html [Last accessed on 2024 Jul [20].

43. Mullins L. Softening of rubber by deformation. *Rubber Chem Technol*. 2012;42(1):339-362.

doi: 10.5254/1.3539210

44. Keating P, Kuo G. Comparison of speaking fundamental

frequency in English and Mandarin. *J Acoust Soc Am*. 2012;132(2):1050.

doi: 10.1121/1.4730893

45. Vlassov S, Oras S, Timusk M, *et al*. Thermal, mechanical, and acoustic properties of polydimethylsiloxane filled with hollow glass microspheres. *Materials (Basel)*. 2022;15(5):1652.

doi: 10.3390/ma15051652

46. Xia Z, Wu X, Yang Q, *et al*. Analysis and test of sound insulation performance of multilayer structures. *Noise Vibr Control*. 2023;43:129-34.

doi: 10.3969/j.issn.1006-1355.2023.06.020

47. Vortice. *Air Handling Unit Catalog*. Vortice. Available from: https://www.vortice.com/media2/export/inglese/doc_pubblicita_catalog_air_handling_unit_122215.pdf [Last accessed on 2020 Jun 27].

48. Xu Y, De la Paz E, Paul A, *et al*. In-ear integrated sensor array for the continuous monitoring of brain activity and of lactate in sweat. *Nat Biomed Eng*. 2023;7(10):1307-1320.

doi: 10.1038/s41551-023-01095-1

49. Burgos CP, Gärtner L, Ballester MAG, *et al*. In-ear accelerometer-based sensor for gait classification. *IEEE Sens J*. 2020;20(21):12895-12902.

doi: 10.1109/jsen.2020.3002589